

Study on the Settlement and Deformation Characteristics of Surrounding Rock of Loess Tunnel

Zunzun Du^{1,*}, Gaolei Hu²

¹College of Geosciences and Engineering, North China University of Water Resources and Electric Power, Zhengzhou, 450046, China

²Zhejiang East China Geotechnical Survey and Design Institute Co., Ltd., Hangzhou, 310012, China

*Corresponding Author Email: 15137832578@163.com

Abstract: There is a water culvert with masonry structure in the mountain of Hanguguan Tunnel. Soil deformation caused by tunnel excavation leads to channel cracking. On the one hand, channel water infiltration leads to loess tunnel collapse, which can easily cause engineering accidents and delay the construction period. On the other hand, it will affect the channel water supply and cause social problems. In this paper, the spatial deformation of the tunnel excavation process in the loess layer is revealed through the settlement of the vault in the tunnel, the monitoring of the convergence of the perimeter, and the force monitoring of the lining support structure of the Hanguguan tunnel, and the influence of the tunnel excavation deformation on the culvert is revealed through numerical calculation. The results show that the arch at the tunnel exit has the largest settlement deformation, the larger cumulative settlement, and the faster settlement rate, and the deformation of the culvert is small, only a millimeter. Compared with the monitoring data, the numerical simulation of tunnel excavation and the vertical settlement are basically consistent with the actual situation.

Keywords: Loess surrounding rock; tunnel surrounding rock; settlement deformation; Excavation deformation.

1. Introduction

With the rapid development of China's transportation infrastructure, hundreds of tunnels with large cross-sections have been built underground, and the loess is decomposed due to structural instability [1], and the loose loess [2] is prone to slippage when the water saturation is high. Loess is a multi-phase porous medium with special structure. When a large-span tunnel or underground space is built on the yellow soil surface, the mechanical action of the loess surrounding the tunnel will be weakened by shear damage of the soil structure, crack, and relax due to deformation development, collapse, and deformation due to immersion damage, and also be affected by some geological conditions such as collapsed caves, cracks, landslides, landslides, etc. In the process of tunnel construction, large deformation, instability, crown collapse, lining fracture, and other failures may be caused, posing a threat to the construction and safe operation of the tunnel [3-8]. The deformation characteristics of the surrounding rock are related to geological conditions, design parameters, construction technology, and management, and there are certain differences. The surrounding rock of the loess foundation has low strength and large deformation, which makes it easy to collapse in engineering construction, resulting in construction delays and casualties. Li et al. [9] reviewed the influence of various heterogeneous factors of rock mass on tunnel displacement. Liu et al. [10] analyzed the effects of three different joint lengths, joint spacing, and joint locations on tunnel failure characteristics. Jia et al. [11] took the Heimagan Tunnel in China as an example to illustrate the variation laws related to surface settlement, deformation, and stress characteristics in shallow buried soft rock tunnels and emphasized the requirements for tunnel support. Shao et al. [12] revealed the formation mechanism of different failures during the construction of loess tunnels through numerical analysis, in which numerical methods were used to simulate the structural characteristics, loess strata, geological

conditions, excavation, and support effects of loess. Based on the "Southward Migration Project from Sanmenxia West to Henan-Shaanxi Border", this paper carries out research on the deformation characteristics, instability mechanism, and deformation control technology of loess surrounding rock, which has great theoretical and practical application value.

2. Project Overview

The Hanguguan Tunnel is located near Beiliwan Village, Lingbao City, Sanmenxia, with the starting and ending stations of the left line of the tunnel ZK119+996~ZK121+950, with a total length of 1954 m, and the starting and ending stations of the right line YK119+996~YK121+984, with a total length of 1988 m. There are 2 cross-vehicular passages and 3 pedestrian crossings in the tunnel, and the left line of the tunnel is set to R=3200 m with a small mileage to a large mileage of 4.394% uphill with a length of 44 m, and then 2.46% downhill with a length of 1910 m. The right line of the tunnel is set as a circular curve with R=3000m from small mileage to large mileage line with 4.394% uphill and 44m in length, and then 2.46% downhill with 1944m in length.

3. Comparative Analysis of Settlement Deformation of the Surrounding Rock

The layout of the settlement displacement monitoring point of the tunnel section is shown in Figure 3-1, and the deformation is monitored in real-time during on-site excavation, and the measurement is stopped after stabilization.

According to the analysis of the monitoring data of 40 selected sections, the summary curves of the settlement measurement data analysis of the tunnel section and the convergence measurement data analysis around the tunnel section are shown in Fig. 3-2, Fig. 3-3, Fig. 3-4 and Fig. 3-5, the resulting data are summarized in Table 3-1.

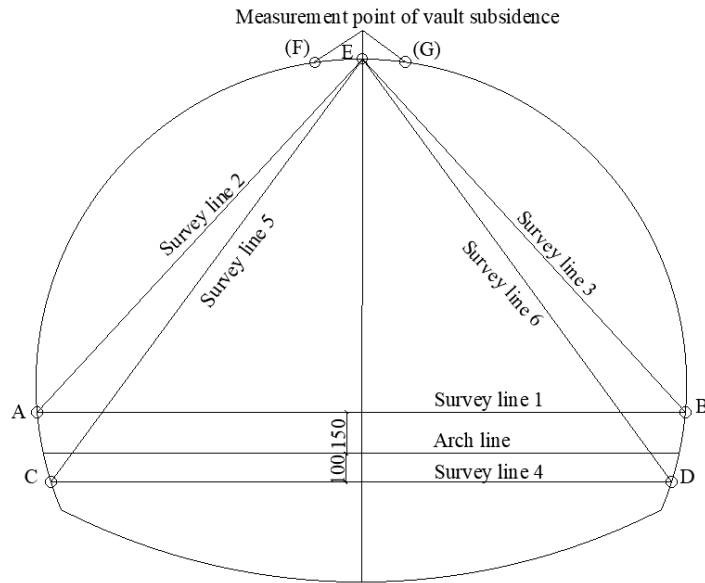


Figure 3-1. Layout of observation points in the cave

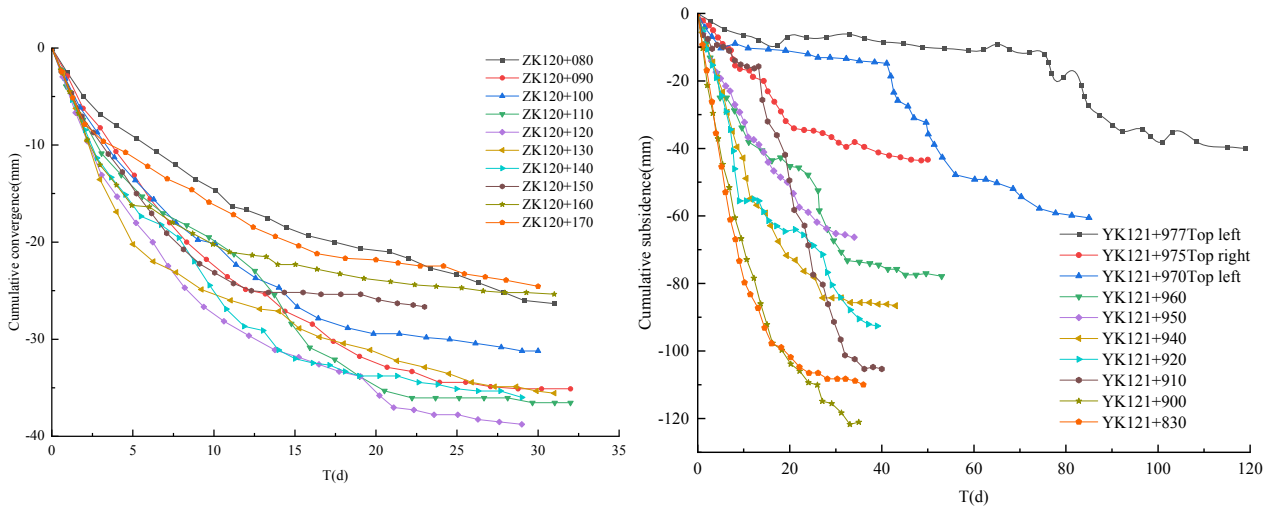


Figure 3-2. Curves of the subsidence of the vault on the left and right lines of the tunnel exit

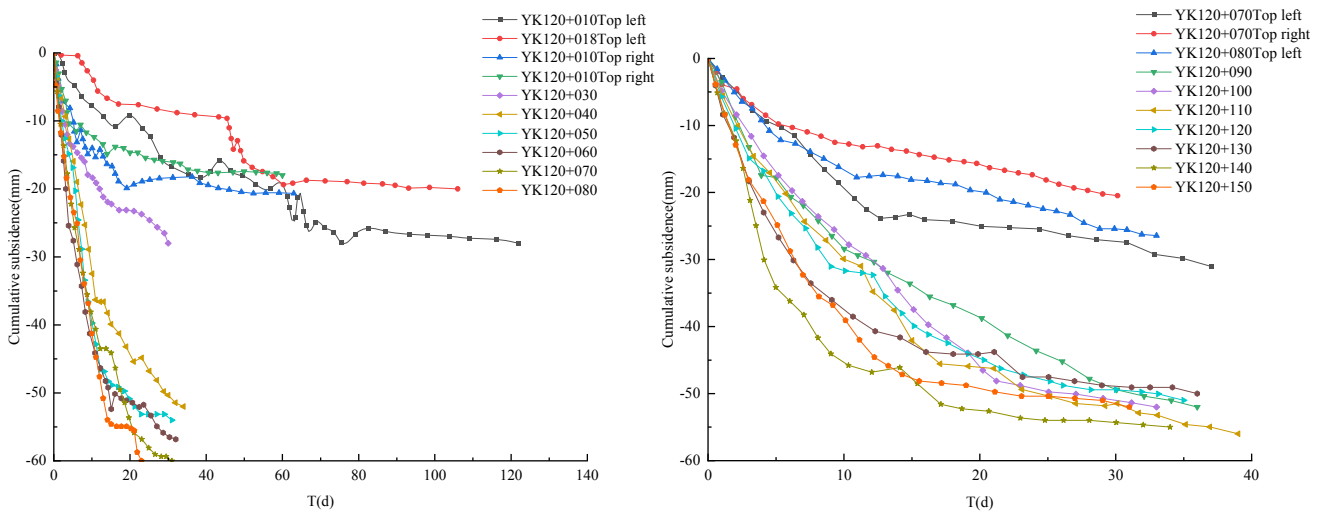


Figure 3-3. Curves of the subsidence of the vault on the left and right lines of the tunnel entrance

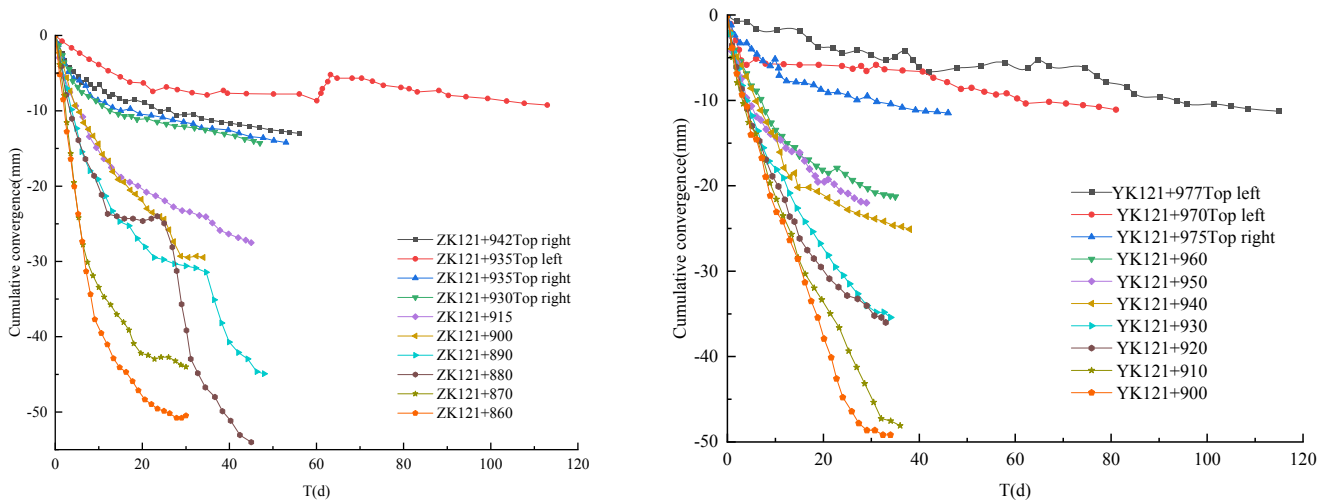


Figure 3-4. Convergence curves around the left and right lines of the tunnel exit

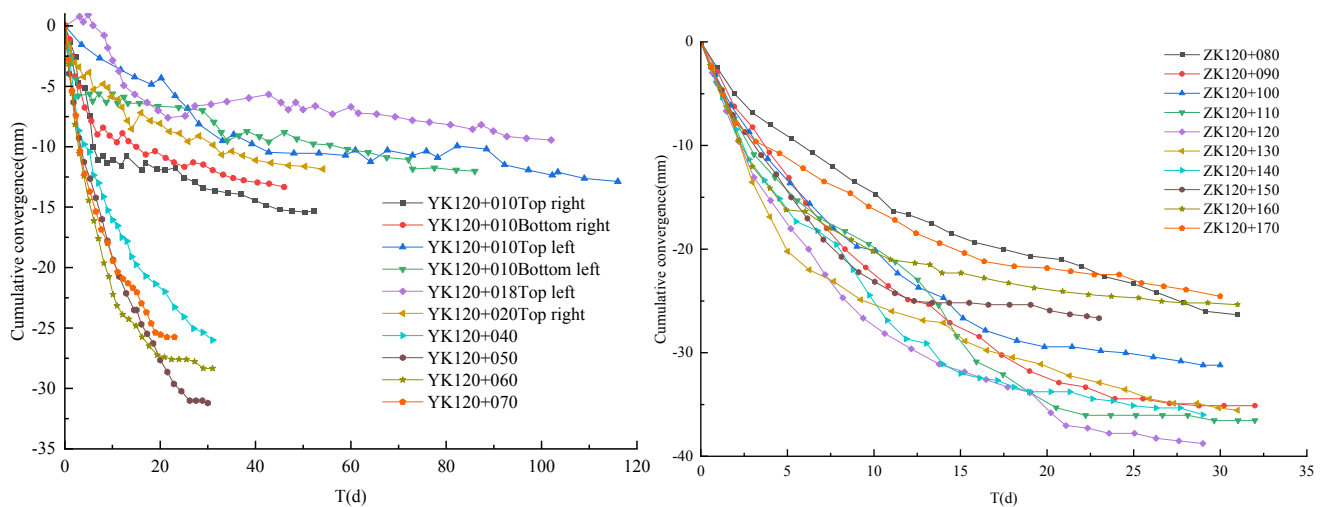


Figure 3-5. Convergence curves around the left and right lines of the tunnel entrance

Table 3-1. Summary of Tunnel Settlement Convergence

Hanguguan Tunnel	Surrounding rock grade	The average amount of subsidence of the vault	The maximum amount of subsidence in the vault	Average Peripheral Convergence	Maximum Peripheral Convergence
Exit the right line	V	80.4	121.7	27.1	49.2
Exit left line	V	55.4	78.9	30.1	58.8
Import right line	V	39.5	59.8	18.6	31.1
Import left line	V	44.4	55.1	31.7	38.7

Through the analysis and comparison of the above charts, it can be found that the settlement deformation of the vault at the exit of the Hanguguan tunnel is the largest, the cumulative settlement is large, and the settlement rate is faster. By comparing the settlement of the vaults on both sides of the exit, it can be found that the settlement on both sides of the outlet is different, and the settlement of the right line is greater than that of the left line, and the settlement speed is also faster. The data shows that the average subsidence of the right-line vault is 80.4 mm, and the maximum cumulative total subsidence reaches 121.7 mm, while the average subsidence of the left-line vault is 55.4 mm, and the maximum cumulative total subsidence is 78.9 mm. Different from the exit, at the entrance of the Hanguguan Tunnel, the settlement

of the arch is relatively small, and the settlement rate is relatively slow. At the inlet, the difference between the sedimentation of the lower left and the lower right is smaller, and the sedimentation is relatively uniform. The data shows that the average settlement of the right line vault is 39.5 mm, and the maximum cumulative total settlement is 59.8 mm, the average settlement of the left line vault is 44.4 mm, and the maximum cumulative total settlement is 55.1 mm. Comparing the convergence around the Hanguguan tunnel section, the numerical values show that the average convergence around the right line section of the tunnel exit is 27.1 mm, and the maximum cumulative convergence value is 49.2 mm, and the average convergence around the left line section is 30.1 mm, and the maximum cumulative convergence value is 58.8 mm.

The cross-section convergence at the inlet is smaller, the convergence rate is slower, and the convergence around the left line is greater than that of the right line. The data shows that the average convergence around the right line section is 18.6 mm, the maximum cumulative convergence value is 31.1 mm, the average convergence amount around the left line section is 31.7 mm, and the maximum cumulative convergence value is 38.7 mm.

4. 3D Model Modeling of Tunnel Culvert Section Excavation

Figure 4-1 is a cross-sectional view of the culvert above the tunnel. According to the known conditions, the model of the culvert section of the Hanguguan Tunnel is roughly established, as shown in Figure 4-2.

For the finite element calculation area, select the mountain and tunnel near the culvert for modeling. 110m along the tunnel direction is the X direction of the calculation model; 150m perpendicular to the tunnel direction is the Y direction of the calculation model; In the vertical direction, 150m from top to bottom is the Z direction. The finite element mesh of the computational model has 71109 elements and 57135 nodes, the model has unidirectional displacement constraints in the X and Y directions, and the bottom surface of the model in the Z direction is a bidirectional displacement constraint. For finite element calculation, the constitutive model of the soil adopts the Mohr-Coulomb model. The culvert under the tunnel is obliquely crossed by the direction of the tunnel route, the oblique angle is 66 degrees, the intersection mileage with the right tunnel is YK121+293.577, and the intersection mileage with the left tunnel is YK121+297.633. At the intersection with the tunnel, the design elevation of the right tunnel is 496.70m, the height difference between the top of the tunnel excavation contour line and the bottom of the tunnel is 28.357m, and the design elevation of the left tunnel is 497.7236m, the height difference between the top of the tunnel excavation contour line and the bottom of the tunnel is 28.054m.

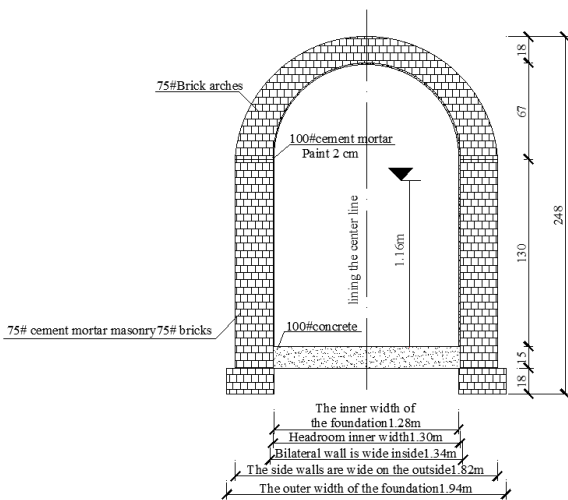


Figure 4-1. Cross-section of the culvert above the tunnel

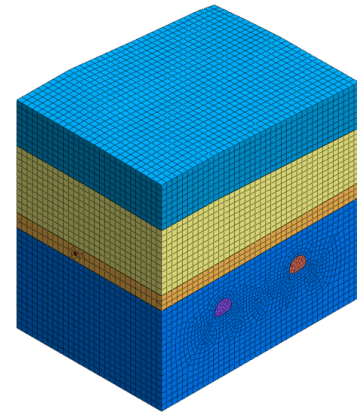


Figure 4-2. Finite element grid diagram of the excavation section of the tunnel culvert

4.1. Tunnel segmented excavation 3D model modeling

In order to better study the stress distribution and deformation law of the surrounding rock in the excavation process of the Hanguguan tunnel, the segmented excavation model was further established in combination with the previous model, and the tunnel's surrounding rock was supported and bolted after each excavation, and the deformation characteristics of the tunnel surrounding rock were further studied, as shown in Figure 4-3 below. Figure 4-4 shows that the model is 200m high, the tunnel direction extends by 40 m, and the finite element mesh of the calculation model has 64,607 elements and 47,769 nodes.

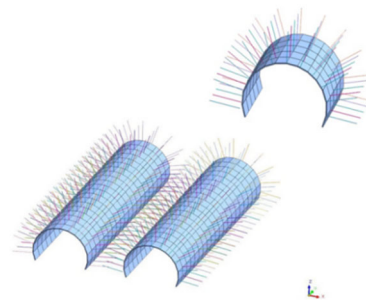


Figure 4-3. Schematic diagram of the initial support and bolt of the tunnel

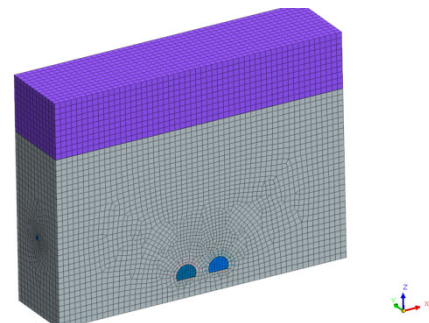


Figure 4-4. A finite element grid diagram of the excavation section of the tunnel culvert

Fig. 4-5 shows the stress and deformation of the tunnel excavation on the underground waterway and the surrounding rock in the absence of lining. When the tunnel is not constructed, due to the influence of its own gravity, its vertical stress increases from 0 to about 2.4MPa. The results show that after the tunnel excavation, the surrounding rock in the

roadway has obvious stress redistribution, as shown in Figure 3-5.

As can be seen from Figures 4-5, due to the construction of the tunnel, the vertical deformation is the largest in the vault position, and the settlement is 67mm. At the bottom of the inverted arch, the bulge amplitude is the largest, with a bulge

amplitude of 43mm.

From Figure 4-6 to Figure 4-7, it can be concluded that the culvert is less affected by the tunnel construction. From the point of view of the deformation caused by tunnel excavation construction, after tunnel construction, the deformation of the culvert is millimeter-level, with slight deformation.

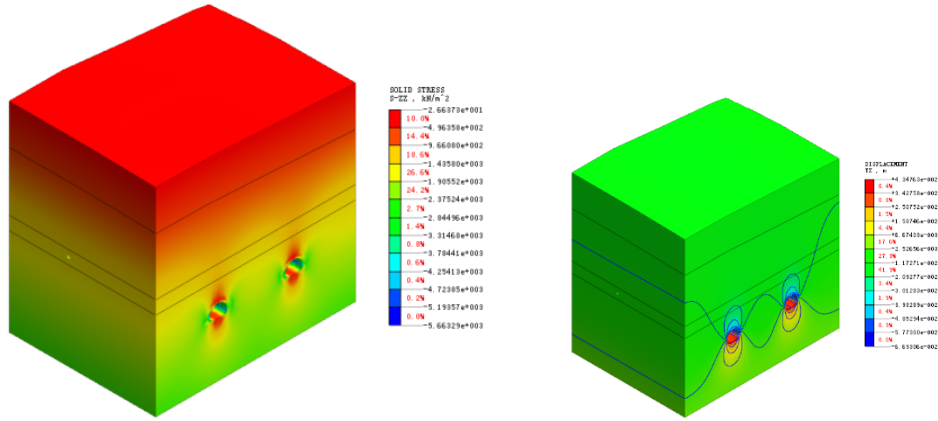


Figure 4-5. Vertical stress and displacement distribution

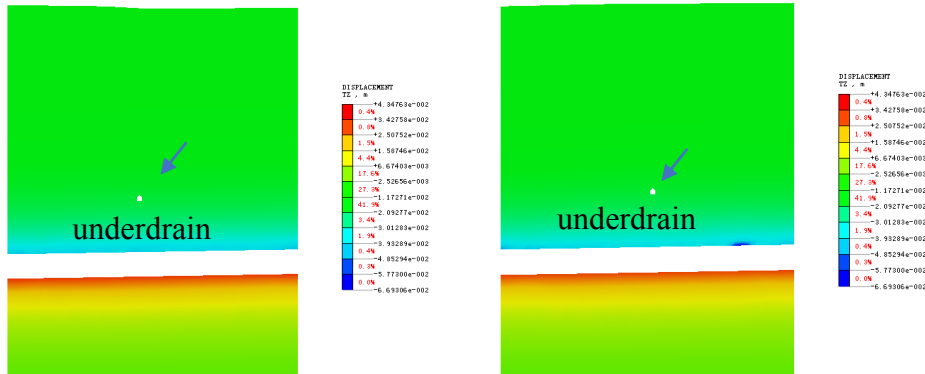


Figure 4-6. Vertical displacement distribution of the longitudinal sections of the left and right lines

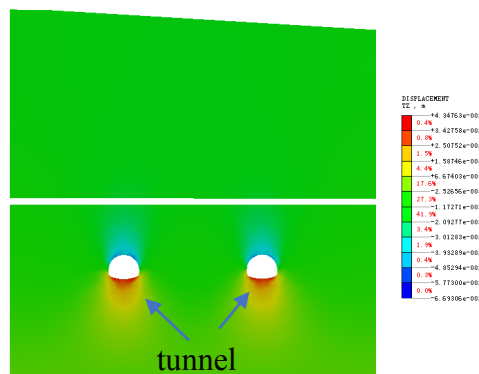


Figure 4-7. Vertical displacement distribution of tunnel cross-section

4.2. Stress and deformation analysis of surrounding rock in tunnel sectional excavation

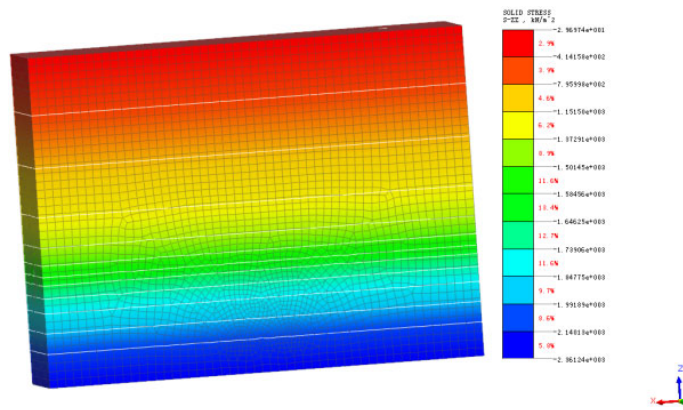
4.2.1. Stress analysis of tunnel surrounding rock

Figure 4-8 shows the vertical stress distribution before tunnel excavation, and Figure 4-9 to Figure 4-11 are the vertical stress distribution of sections 1, 5, and 20 during tunnel excavation, respectively. By observing the stress distribution diagram in the original state, it can be seen that the stress in the buried depth of the tunnel is 2.3~2.4MPa.

After the first stage of tunnel excavation, the stress near the tunnel was redistributed, and the maximum stress was concentrated on both sides of the tunnel's initial lining, which was about 5MPa, as shown in Figure 4-9. Through the analysis, it is found that the soil can be effectively strengthened through pre-lining and bolt reinforcement, and the large displacement and deformation of the surrounding rock can be avoided. Figures 4-10 and 4-11 are the tunnel stress distribution diagrams of the fifth and final stages of tunnel excavation, respectively. The analysis shows that with further excavation of the tunnel, the stress distribution state of

the tunnel gradually changes, and the pressure on both sides of the tunnel lining gradually increases and finally reaches

about 6 MPa, and the stress of the surrounding rock at the top of the tunnel is about 2MPa.



4.2.2. Vertical deformation analysis of tunnel surrounding rock

Figure 4-12 is the initial state before excavation, the vertical displacement in the process of segmented excavation from Figure 4-13 to Figure 4-15, after the first stage of excavation and support, the vertical displacement distribution map of the first section of tunnel excavation in Figure 4-13 can be obtained that the vertical displacement of the top of the tunnel after stabilization is 28 mm, and the tunnel road surface is uplifted by 22mm. According to the vertical displacement

distribution map of the fifth section of tunnel excavation in Figure 4-14, it can be concluded that the vertical displacement is 59.6mm and the tunnel pavement uplift is 78.9mm after the support is stabilized. The vertical displacement distribution of the final section (20) of tunnel excavation through Figure 4-15 is 63.2mm, and the tunnel pavement uplift is 78.6mm. Through comparative analysis with the monitoring data, the vertical settlement is basically consistent, and the tunnel tends to be stable after support, which meets the specifications and engineering requirements.

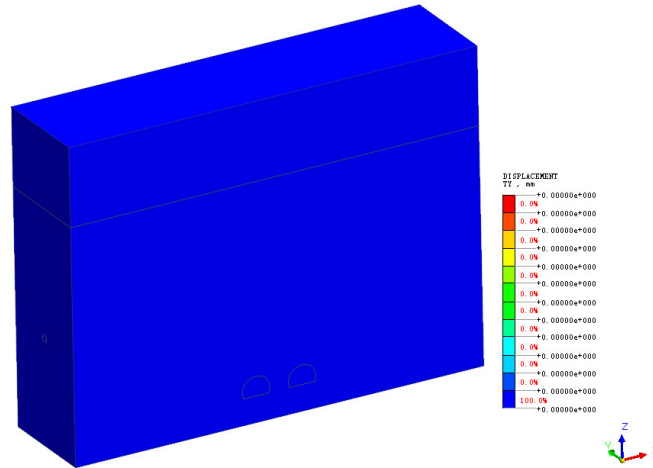


Figure 4-12. The original state of the vertical displacement before the tunnel is excavated

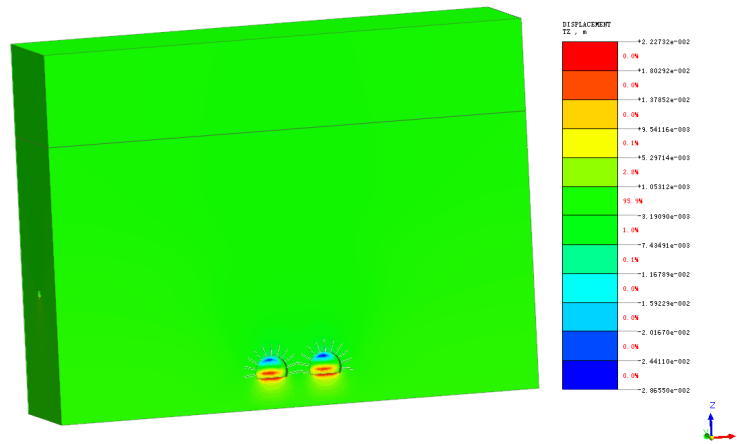


Figure 4-13. Vertical displacement distribution of the first section of tunnel excavation

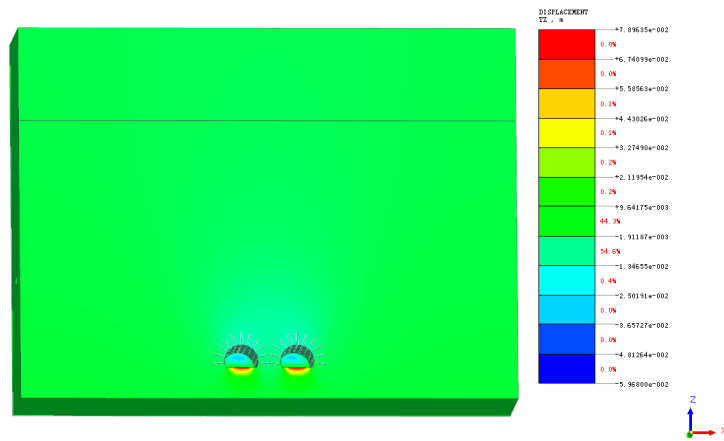


Figure 4-14. Vertical displacement distribution of the fifth section of tunnel excavation

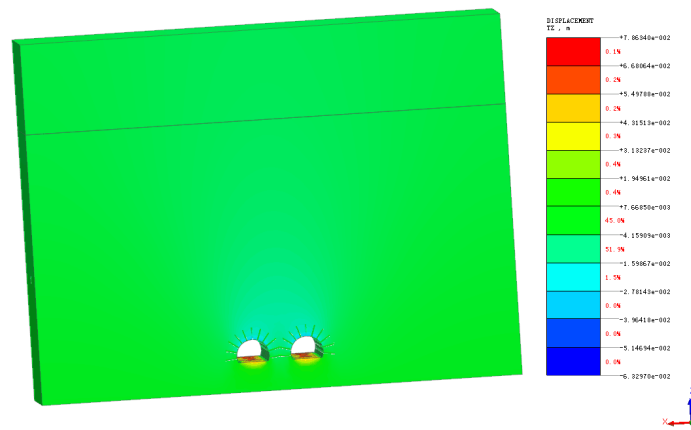


Figure 4-15. Vertical displacement distribution of the final section (20) of tunnel excavation

5. Conclusion

(1) Through the analysis of the settlement deformation data of 40 sections of the Hanguan Tunnel, the settlement deformation of the vault at the exit of the Hanguan Tunnel is the largest, the cumulative settlement amount is large, and the settlement rate is faster. The average settlement of the right line vault of the outlet is 80.4mm and the maximum cumulative settlement is 121.7mm, and the average settlement of the left line vault is 55.4mm and the maximum cumulative settlement is 78.9mm. The average settlement of the inlet right-line vault is 39.5mm, the maximum cumulative total settlement is 59.8mm, and the average settlement of the left-line vault is 44.4mm, and the maximum cumulative total settlement is 55.1mm. The average convergence around the right line section of the tunnel exit is 27.1mm, the maximum cumulative convergence value is 49.2 mm, the average convergence around the left line section of the exit is 30.1mm, and the maximum cumulative convergence value is 58.8mm. The average convergence around the right line section of the inlet is 18.6mm, the maximum cumulative convergence value is 31.1mm, the average convergence value around the left line section is 31.7mm, and the maximum cumulative convergence value is 38.7mm.

(2) Through finite element numerical simulation, the deformation of the culvert after tunnel construction is analyzed. Numerical calculations show that the deformation of the culvert is small, only a millimeter. The vertical displacement distribution map of the first section of tunnel excavation can be obtained, and the vertical displacement of the top of the tunnel and the uplift of the tunnel pavement is 22mm after stabilization. After the final section of tunnel excavation (20 sections) was excavated and supported, the vertical settlement displacement was 63.2mm, and the tunnel pavement was uplifted by 78.6mm. Comparing it with the monitoring data, the results show that the vertical settlement is basically consistent with the actual situation, and the tunnel tends to be stable after support, meeting the specifications and engineering requirements.

References

- [1] Wen B.-P. And Yan Y.-J. "Influence of structure on shear characteristics of the unsaturated loess in Lanzhou", China, *Engineering Geology*, (2014) 168, 46–58. <https://doi.org/10.1016/j.enggeo.2013.10.023>
- [2] Shao S. J, Wang L. Q, Shao S, and Wang Q. "Structural yield and collapse deformation of loess", *Chinese Journal of Geotechnical Engineering*, (2017) 39, no. 8, 1–9.
- [3] Tonon F. "ADECO full-face tunnel excavation of two 260m² tubes in clays with sub-horizontal jet-grouting under minimal urban cover", *Tunnelling and Underground Space Technology*, (2011) 26, no. 2, 253–266. <https://doi.org/10.1016/j.tust.2010.09.006>
- [4] Graziani A. And Boldini D. "Remarks on axisymmetric modeling of deep tunnels in argillaceous formations", *Tunnelling and Underground Space Technology*, (2012) 28, 70–79. <https://doi.org/10.1016/j.tust.2011.09.006>
- [5] Ng C. W. W, Hong Y, Liu G. B, and Liu T. "Ground deformations and soil-structure interaction of a multi-propped excavation in Shanghai soft clays", *Géotechnique*, (2012) 62, no. 10, 907–921. <https://doi.org/10.1680/geot.10.p.072>
- [6] Lisjak A, Garitte B, and Grasselli G. "The excavation of a circular tunnel in a bedded argillaceous rock (Opalinus Clay): short-term rock mass response and FDEM numerical analysis", *Tunnelling and Underground Space Technology*, (2012) 45, 227–248. <https://doi.org/10.1016/j.tust.2014.09.014>
- [7] Assallay A. M, Rogers C. D. F, and Smalley I. J. "Formation and collapse of metastable particle packings and open structures in loess deposits", *Engineering Geology*, (1997) 48, no. 1-2, 101–115. [https://doi.org/10.1016/s0013-7952\(97\)81916-3](https://doi.org/10.1016/s0013-7952(97)81916-3)
- [8] Vietor A. M, Rogers C. D. F, and Smalley I. J. "Formation and collapse of metastable particle packings and open structures in loess deposits", *Engineering Geology*, (1997) 48, no. 1-2, 101–115. [https://doi.org/10.1016/s0013-7952\(97\)81916-3](https://doi.org/10.1016/s0013-7952(97)81916-3)
- [9] Li, G, He, M. & Bai, Y. "The influence of the heterogeneity of rock mass for surrounding rock stability evaluation of a tunnel" *Bull Eng Geol Environ* 82, 144 (2023). DOI: 10.1007/s10064-023-03145-z
- [10] Liu, Wanrong, Peng, Chao, Zhang, Baoliang. "Study on Influence of Joint Distribution on Surrounding Rock Failure of an Underground Tunnel", *Geofluids*, 2021, 3621040, 12 pages, 2021. DOI: 10.1155/2021/3621040
- [11] Jia J, Xi B, Wang X, Tenorio VO, Liu Z. "A Study on Deformation Characteristics and Stability of Soft Surrounding Rock for a Shallow-Buried Tunnel", *Applied Sciences*, 2024; 14(14):6014. DOI: 10.3390/app14146014
- [12] Shao Shuai, Shao Shengjun, Li Jun, Qiu Bing. "An Analysis of Loess Tunnel Failure and Its Mechanism", *Advances in Civil Engineering*, 2021, 6671666, 18 pages, 2021. DOI: 10.1155/2021/6671666